ASCE
AMERICAN SOCIETY OF CIVIL ENGINEERS

September 2013 • Volume 139, Number 9
ISSN 0733-9429 • CODEN: JHEND8

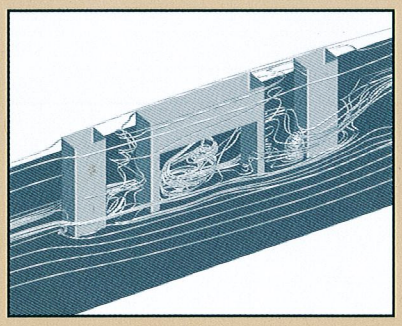

Journal of Hydraulic Engineering

EWRI
ASCE
ENVIRONMENTAL & WATER RESOURCES INSTITUTE

Implicit TVDLF Methods for Diffusion and Kinematic Flows

A. M. Wasantha Lal, M.ASCE[1]; and Gabor Toth[2]

Abstract: Diffusion-wave and kinematic-wave approximations of the St. Venant equations are commonly used in physically based, regional hydrologic models because they have high computational efficiency and use fewer equations. Increasingly, models based on these equations are being applied to cover larger areas of land with different surface and groundwater regimes and complicated topography. Existing numerical methods are not well suited for multiyear simulation of detailed flow behavior unless they can be run efficiently with large time steps and control numerical error. A numerical method also should be able to solve both diffusive and kinematic wave models. A total variation diminishing Lax-Friedrichs type method (TVDLF) that is stable and accurate with both diffusive- and kinematic-wave models and large time steps is presented as a means to address this problem. It uses a linearized conservative implicit formulation that makes it possible to avoid nonlinear iterations. The numerical method was tested successfully using steady flow profiles, analytical solutions for wave propagation, and observed data from a field experiment in a mountain stream of Sri Lanka. A grid convergence test and an error analysis are carried out to determine how the model errors of the numerical schemes behave with the discretization. **DOI: 10.1061/(ASCE)HY.1943-7900.0000749.** © *2013 American Society of Civil Engineers.*

CE Database subject headings: Numerical models; Kinematics; Field tests; Sri Lanka.

Author keywords: Implicit total variation diminishing Lax-Friedrichs (TVDLF); Kinematic flow; Diffusion wave.

Introduction

Numerical models based on the diffusive-wave approximation of the St. Venant equations provide a stable, accurate and efficient way to solve most canal and river flow problems when the inertia terms are negligible. Such models are useful when simulating regional flow over large physical spaces, such as south Florida, with many thousands of miles of canals, and 30-year to 40-year simulation periods. Diffusion-wave models are efficient for these applications because only one equation has to be solved per river segment for head instead of two as in the case of full St. Venant equations. The run times of these models can be kept low by using implicit solution methods and efficient linear equation solvers. Commonly used diffusive-wave formulations include the fully implicit formulation by Akan and Yen (1981); the explicit formulation by Hromadka et al. (1987) and the noniterative implicit formulation by Lal (1998). Integrated physically based models such as MIKE-SHE use variants of these methods in two dimensions (Graham and Butts 2005).

Formulation of the diffusive-wave model commonly involves central-differencing. This formulation can be fast and accurate when flow is diffusive, but fail under a number of conditions found in large hydrologic systems with both one-dimensional and two-dimensional flow. This formulation can be inaccurate when the inertia terms are too large, as described by Ponce et al. (1978). The fully implicit formulation of the diffusive-wave model (Akan and Yen 1981) is generally stable with large time steps. Such a formulation can, however, fail to converge when attempting to couple a one-dimension (1D) model with a large two-dimension (2D) flow model, when the bottom topography is too uneven, or when there is wetting and drying. A noniterative implicit formulation, on the other hand, does not have this problem because it does not need iterations. However, this method is subject to larger numerical errors, visible oscillations, and dry-outs when the bottom slope is relatively steep and the flow is kinematic. Many of these problems are due to the inability of central-difference–based diffusive-wave models to simulate kinematic flow, which is governed by hyperbolic partial-differential equations. Adopting a purely kinematic-wave model is also not possible because of the need to simulate diffusive conditions in other parts of the domain. More details on various kinematic- and diffusive-flow methods can be found in Ponce (1991) and Singh (1996).

The total variation diminishing Lax-Friedrichs (TVDLF) formulation with first-order or second-order spatial accuracy can be used to solve both diffusive- and kinematic-wave models. The use of this method is critical when solving 1D canal flow problems coupled with 2D surface and groundwater flow systems without iterations. This method has been explained in detail by Yee (1989), and used by Toth and Odstrcil (1996) and Toth et al. (1998). It falls under a class of linearized conservative implicit solution methods that is popular in computational fluid dynamics (CFD) and magneto hydrodynamics (MHD). The method is used extensively to solve nonlinear hyperbolic-parabolic problems. Extra features used in the implementation include the capability to calculate the Jacobian numerically or analytically, and the capability to achieve second-order spatial accuracy by modifying the flux function.

In the case of south Florida, the TVDLF method is useful in improving the existing noniterative method used to simulate the south Florida system (Lal et al. 2005), and making sure that both flat and steep slopes can be simulated simultaneously in one model. The existing method is adequate for both 1D and 2D wetland conditions close to the southern part of Florida and the Everglades, but gets into numerical difficulties when simulating certain areas in the

[1]Principal Engineer, South Florida Water Management District, 3301 Gun Club Rd., West Palm Beach, FL 33406 (corresponding author). E-mail: wlal@sfwmd.gov

[2]Research Scientist, Univ. of Michigan, Ann Arbor, MI 48109. E-mail: gtoth@umich.edu

Note. This manuscript was submitted on February 1, 2012; approved on February 19, 2013; published online on February 21, 2013. Discussion period open until February 1, 2014; separate discussions must be submitted for individual papers. This paper is part of the ***Journal of Hydraulic Engineering***, Vol. 139, No. 9, September 1, 2013. © ASCE, ISSN 0733-9429/2013/9-974-983/$25.00.

northern parts of the state. Flow in the Everglades can be diffusive, while flow in the north can be kinematic. The method currently used can use 6-h to 24-h time steps when simulating relatively flat areas and 1- to 60-minute time steps when simulating steep areas. When the TVDLF method is used, the time step restriction for kinematic flow becomes relaxed, and the need for iterative coupling between 1D and 2D coupling goes away. Some of the challenges faced during a similar 1D and 2D coupling exercise between the HEC-RAS and MODFLOW models can be found in the paper by Rodriguez et al. (2008).

The TVDLF formulation introduced in this paper was tested extensively to ensure accurate solutions throughout a wide range of flow and bottom slope conditions, and a wide range of spatial and temporal discretizations (Lal 2008). The first-order accurate TVDLF solution is compared to a fourth-order accurate Runge-Kutta solution under various steady-state conditions and spatial discretizations. A grid convergence test is carried out to make sure that as the discretization gets finer, the numerical solution approaches the true solution. The method is then tested under various kinematic and diffusive conditions to make sure that the wave speeds and wave attenuations compare well with analytical solutions and with the solutions obtained using existing methods such as those used by Akan and Yen (1981), and Lal (1998). In addition, a field experiment was conducted on the Dambulu River of Sri Lanka to test the TVDLF method in a natural river. During the experiment, sinusoidal discharge waves were generated at the upstream end of the river using an existing gated structure, and the water levels observed at various downstream locations were compared to the results of the TVDLF method and the analytical equations. The objective of this experiment was to make sure that both the governing equations and the numerical formulation could simulate the flow in naturally-occurring steep rivers.

In order to determine the amplitude and phase errors of the TVDLF solution, a numerical experiment is carried out using a simplified version of the field experiment, assuming a uniformly sloping canal. This simplification allows the creation of an analytical solution that is useful in calculating the numerical error. The numerical experiment is useful in understanding how both amplitude and phase errors vary with the discretization in both diffusive-wave and kinematic-wave models. The paper shows that the implicit TVDLF method can be used to solve a range of flow problems using many levels of spatial and temporal discretizations.

Governing Equations

River flow or canal flow can be described using the St. Venant equations, which consist of a continuity equation and a momentum equation. The equations can be written for a wide river using the water depth h and the discharge per unit width q as primitive variables:

$$\frac{\partial h}{\partial t}+\frac{\partial q}{\partial x}=0 \tag{1}$$

$$\frac{\partial q}{\partial t}+\frac{\partial}{\partial x}\left(\frac{q^2}{h}\right)+gh\left(s_f+\frac{\partial h}{\partial x}-s_0\right)=0 \tag{2}$$

where g = gravitational acceleration; $s_0=-\partial z/\partial x$ = river bed slope; z = river bottom elevation; $q=uh$ = while $h>0$; u = average flow velocity; s_f = friction slope in Manning's equation written as

$$q=\frac{1}{n_b}h^{1+\gamma}|s_f|^{\alpha}\mathrm{sgn}(s_f) \tag{3}$$

where $\mathrm{sgn}(s_f)=\pm 1$ depending on $s_f>0$ or $s_f<0$; $\gamma=2/3$; $\alpha=1/2$; n_b = Manning's constant. Values of γ and α vary for wetlands and other applications. Values for these parameters for wetlands can be found in Kadlec and Wallace (2009).

The diffusive wave or no inertia approximation of the St. Venant equation is established by neglecting the inertia terms of the momentum equation. These are the first two terms of Eq. (2). In the diffusive wave model, Eq. (2) collapses to $s_f=s_H$, where $s_H=-\partial H/\partial x$ = water surface slope; $H=h+z$ = water level. In the case of kinematic flow, friction slope is equal to the bottom slope or $s_f=s_0$. The numerical method developed below is for the no inertia approximation of the St. Venant equations.

Before developing a numerical method, Eqs. (1)–(3) are combined to produce the following linearized advection-diffusive equation assuming that $q=q(h,s_H)$:

$$\frac{\partial h}{\partial t}+c\frac{\partial h}{\partial x}=K\frac{\partial^2 h}{\partial x^2} \tag{4}$$

where

$$c=\frac{\partial q}{\partial h}=(1+\gamma)\frac{1}{n_b}h^{\gamma}|s_H|^{\alpha}\mathrm{sgn}(s_H)=(1+\gamma)\frac{q}{h} \tag{5}$$

$$K=\frac{\partial q}{\partial s_H}=\alpha\frac{1}{n_b}h^{1+\gamma}|s_H|^{\alpha-1}=\alpha\frac{q}{s_H} \tag{6}$$

Here, c is the kinematic celerity and K is the hydraulic diffusivity. When the depth is small and the slope is steep, the term with c dominates and the equation becomes predominantly hyperbolic. When the depth is large and the slope is small, the term with K dominates and the equation becomes predominantly parabolic. The singularity of K at $s_H=0$ is avoided in the numerical method, as shown later. In the case of the hyperbolic equations, an oscillation-free method is needed to obtain a solution, while in the case of the parabolic equations, a central-difference–based implicit method is generally sufficient.

The conditions for applying kinematic and diffusive wave models were derived by Ponce et al. (1978). These conditions are useful whenever approximate formulations of the St. Venant equation are used. The kinematic model is applicable when $Ps_0u_n/h_n>171$ where P = propagation period; s_0 = channel bed slope; u_n = uniform flow velocity; h_n = uniform flow depth. The diffusive wave model is applicable when $Ps_0\sqrt{(g/h_n)}>30$ where g = gravitational acceleration.

Numerical Solution

The numerical formulation of the diffusive wave model involves solving the scalar conservative Eq. (1) using a first-order implicit finite volume formulation. For a river segment, the finite volume formulation can be written as

$$\frac{h_i^{n+1}-h_i}{\Delta t}=\frac{1}{\Delta x}(q^m_{i-(1/2)}-q^m_{i+(1/2)})=R_i(\mathbf{h}^m) \tag{7}$$

where the superscripts n and $n+1$ correspond to time levels n and $n+1$, respectively; $q^m_{i+1/2}$ is the numerical flux function at segment joint $i+1/2$ at time level m defined later; $R_i(\mathbf{h}^m)$ is used to represent the right hand side of Eq. (7); $\mathbf{h}$ is the vector of water depths $[h_1,h_2,\ldots,h_N]^T$; N = number of canal segments in the model. Fig. 1 shows a definition sketch.

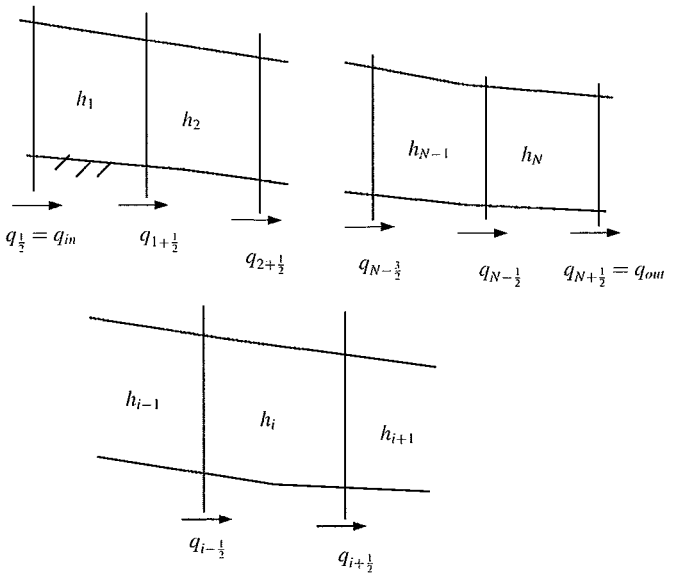

Fig. 1. Definition sketch of a discretized river in 1D

Flux Function for Central-Difference–Based Methods

Some of the popular numerical models based on the diffusive wave assumption can be explained using Eq. (7) and various approximate forms of $q^m_{i+1/2}$:

$$q^m_{i+(1/2)} = K^{n_1}_{i+(1/2)}\left(\frac{h_i + z_i - h_{i+1} - z_{i+1}}{\Delta x_{i+\frac{1}{2}}}\right)^{n_2}$$

$$\text{where } K^{n_1}_{i+(1/2)} = \left[\frac{1}{n_b} h^{1+\gamma} s_H^{\alpha-1}\right]^{n_1}_{i+(1/2)} \tag{8}$$

with $s_H = \max(|s_{i+(1/2)}|, \delta_H)$ when $\alpha < 1$; $s_{i+(1/2)} = (H_i - H_{i+1})/\Delta x_i$; $\delta_H \approx 10^{-9}$ is suitable for applications in south Florida. Variables n_1 and n_2 represent time levels that determine if the method is explicit or implicit, as described below. Three of the formulations using this flux function are described as follows:

1. Explicit method: Formulation (7) becomes explicit when $n_1 = n_2 = n$ (Hromadka et al. 1987). The EXTRAN module of the storm water management model (Rosner et al. 1984) also uses this method. With explicit methods, h_i^{n+1} in Eq. (7) can be obtained using Eq. (8). The fully explicit formulation requires small time steps which slow down model runs.
2. The fully implicit method (Akan and Yen 1981): The formulation becomes implicit when $n_1 = n_2 = n + 1$. The MIKE-SHE model (Graham and Butts 2005) and a number of commonly used overland flow models use a 2D version of this method. With this method, Eq. (7) becomes a nonlinear system of equations that has to be solved simultaneously. A strict time step restriction is not needed for implicit methods. But Newton's method with iterations is required to solve this problem. The convergence of this method is slow especially when slope s_H is very small ($<10^{-9}$ when using double precision arithmetic) or when the topography is uneven. Some large scale regional model applications require thousands of iterations before convergence. Nonconvergence is also possible with this method.
3. The noniterative implicit method: The nonlinear formulation with $n_1 = n$ and $n_2 = n + 1$ can be solved noniteratively and with approximate Jacobians when the flow is changing slowly. This method, explained by Lal (1998), is faster because of the use of the implicit formulation with no iterations. This is an important advantage when solving large coupled hydrologic systems. But the solution is oscillatory when the slopes are steep unless small time steps are used. This method becomes unstable with large systems even before implicit methods are used.

TVDLF Methods

The TVDLF method described by Yee (1987) and Toth et al. (1998) can overcome many of the problems in central-difference–based methods described in the previous section. It uses a conservative linearized implicit method and therefore does not need Newton's iterations. In order to ensure that the solution to Eq. (7) remains oscillation free and positive in h when the equation becomes predominantly hyperbolic, the authors use a total variation diminishing (TVD) flux function. The TVD property was introduced by Harten (1983) to control or prevent the generation of spurious oscillations in numerical solutions to hyperbolic problems. The flux function $q_{i+(1/2)}$ in Eq. (7) giving the TVD property is defined as

$$q_{i+(1/2)} = \frac{1}{n_b} h^{\gamma+1}_{i+(1/2)} |s_{i+(1/2)}|^{\alpha} \text{sgn}(s_{i+(1/2)}) - \frac{1}{2}|c_{i+(1/2)}|(h_{i+1} - h_i) \tag{9}$$

where $h_{i+(1/2)} = \max[0, 0.5(h_i + h_{i+1})]$. The second term represents numerical flux required for maintaining the TVD property. The value of celerity $c_{i+(1/2)}$ is calculated as

$$c_{i+(1/2)} = (1+\gamma)\frac{1}{n_b} h^{\gamma}_{i+(1/2)} |s_{i+(1/2)}|^{\alpha} \text{sgn}(s_{i+(1/2)}) \tag{10}$$

The flux is considered to be positive when moving water from i to $i + 1$. The flux function can be computed at n or $n + 1$ time levels to give explicit and implicit methods. Eq. (9) gives only the first-order flux.

A second-order accurate solution in space can be obtained using modified heads with the same function. These modified heads are defined as

$$h^*_i = h_i + 0.5\Delta h^*_i \tag{11}$$

$$h^*_{i+1} = h_{i+1} - 0.5\Delta h^*_{i+1} \tag{12}$$

where the limited slope Δh^*_i is defined as

$$\Delta h^*_i = [0.5\,\text{sgn}(\Delta h_i) + 0.5\,\text{sgn}(\Delta h_{i+1})]\min(\beta|\Delta h_i|, \beta|\Delta h_{i+1}|, 0.5|\Delta h_i + \Delta h_{i+1}|) \tag{13}$$

and $\Delta h = h_i - h_{i-1}$; β is a tuned parameter used in the slope limiting function subject to $1 < \beta < 2$ (van Leer 1979). The parameter β is a problem dependent parameter that gives some control over the error. For the current problem, larger β values provide better accuracy and smaller β values provide better stability.

Implicit Solution Scheme for TVDLF Method

Various implicit methods described earlier with fluxes in Eq. (7) defined at time step $m = n + 1$ can be solved using Newton's method. It can be shown that the solution involves determining the vector $\Delta\mathbf{h}$ in

$$\left[\mathbf{I} - \frac{\partial \mathbf{R}(\mathbf{h})}{\partial \mathbf{h}} \Delta t\right]^n \cdot \Delta \mathbf{h} = \mathbf{R}(\mathbf{h}^n) \Delta t \tag{14}$$

where $\mathbf{h} = [h_i, h_2, \ldots h_N]^T$ = vector of water depths; $\mathbf{R}$ is defined in (7); $\mathbf{I}$ = identity matrix. The vector of water depths is updated at every time step using $\mathbf{h}^{n+1} = \mathbf{h}^n + \Delta \mathbf{h}$. No iterations are used with the TVDLF method. The Jacobian $\partial \mathbf{R}(\mathbf{h})/\partial \mathbf{h}$ at the time level n is calculated numerically or analytically. In either case, (14) for a 1D problem can be written as a tri-diagonal system of equations for $i = 1, N$:

$$A_i \Delta h_{i-1} + B_i \Delta h_i + C_i \Delta h_{i+1} = R_i \Delta t \tag{15}$$

The Thomas algorithm is useful in solving the linear equations resulting from this approach. The matrix elements A_i, B_i, and C_i in the three nonzero diagonals of the Jacobian can be calculated analytically or numerically. For $i = 2, N-1$, the nonzero matrix elements can be calculated using

$$A_i = -\frac{\Delta t}{\Delta x} \frac{\partial q_{i-1/2}}{\partial h_{i-1}}, \qquad B_i = 1 - \frac{\Delta t}{\Delta x}\left(\frac{\partial q_{i-1/2}}{\partial h_i} - \frac{\partial q_{i+1/2}}{\partial h_i}\right) \tag{16}$$

$$C_i = +\frac{\Delta t}{\Delta x} \frac{\partial q_{i+1/2}}{\partial h_{i+1}}, \qquad R_i = \frac{q_{i-1/2} - q_{i+1/2}}{\Delta x} \tag{17}$$

At the boundaries,

$$B_1 = 1 - \frac{\Delta t}{\Delta x}\left(\frac{\partial q_{\text{in}}}{\partial h_1} - \frac{\partial q_{3/2}}{\partial h_1}\right), \qquad C_1 = +\frac{\Delta t}{\Delta x} \frac{\partial q_{3/2}}{\partial h_1} \tag{18}$$

$$B_N = 1 - \frac{\Delta t}{\Delta x}\left(\frac{\partial q_{N-1/2}}{\partial h_N} - \frac{\partial q_{\text{out}}}{\partial h_N}\right), \qquad A_N = -\frac{\Delta t}{\Delta x} \frac{\partial q_{N-1/2}}{\partial h_N} \tag{19}$$

$$R_1 = \frac{q_{\text{in}} - q_{3/2}}{\Delta x}, \qquad R_N = \frac{q_{N-1/2} - q_{\text{out}}}{\Delta x} \tag{20}$$

At the upstream boundary, $q_{\text{in}}(h_1)$ represents inflow, and at the downstream boundary, $q_{\text{out}}(h_N)$ represents outflow, both formulated for the appropriate boundary condition types.

Calculation of Jacobian Using Analytical Method

The terms of the Jacobian $\partial q_{i+1/2}/\partial h_i$ and $\partial q_{i+1/2}/\partial h_{i+1}$ required to calculate the terms of Eqs. (16)–(20) can be obtained using Eq. (9) where $q_{i+1/2} = q_{i+1/2}(h_{i+1/2}, s_{i+1/2})$. Applying the chain rule for the TVDLF method, it can be shown that

$$\frac{\partial q_{i+(1/2)}}{\partial h_i} = \frac{1}{2} c_{i+(1/2)} + \frac{1}{\Delta x} K_{i+(1/2)} + \frac{1}{2}|c_{i+(1/2)}| - \frac{1}{2}\frac{h_{i+1} - h_i}{h_{i+(1/2)}}\left[\frac{1}{2}\gamma |c_{i+(1/2)}| - \frac{1}{\Delta x}(1+\gamma) K_{i+(1/2)} \text{sgn}(s_{i+(1/2)})\right] \tag{21}$$

$$\frac{\partial q_{i+1/2}}{\partial h_{i+1}} = \frac{1}{2} c_{i+1/2} - \frac{1}{\Delta x} K_{i+1/2} - \frac{1}{2}|c_{i+1/2}| - \frac{1}{2}\frac{h_{i+1} - h_i}{h_{i+1/2}}\left[\frac{1}{2}\gamma |c_{i+1/2}| + \frac{1}{\Delta x}(1+\gamma) K_{i+1/2} \text{sgn}(s_{i+(1/2)})\right] \tag{22}$$

The value of $c_{i+1/2}$ is calculated using (10). The value of $K_{i+1/2}$ is calculated as

$$K_{i+1/2} = \alpha h_{i+1/2}^{1+\gamma} \frac{1}{n_b} \frac{|s_{i+1/2}|^\alpha}{(|s_{i+1/2}| + \delta_s)} \tag{23}$$

where $\delta_s = 1.0 \times 10^{-9}$ for most problems within south Florida where the slopes in the wetlands can be as low as 2×10^{-5} to 5×10^{-5}. The term $|s_{i+1/2}|^\alpha/(|s_{i+1/2}| + \delta_s)$ prevents division by zero when the slope is small. An alternative form is $|s_{i+1/2}|^\alpha/(\max(|s_{i+1/2}|, \delta_s)$. If the selected value of δ_s is too small there can be nonconvergence.

Calculation of Jacobian Using Numerical Derivatives

The Jacobian in Eq. (14) can also be calculated numerically using

$$\frac{\partial R_i}{\partial h_j} = \frac{R_i(h_1, \ldots, h_j + \epsilon, \ldots, h_N) - R_i(\mathbf{h})}{\epsilon} \tag{24}$$

where $R_i(\mathbf{h})$ represents the right hand side of Eq. (7). The value of ϵ used is the typical magnitude of h multiplied by the square root of machine precision of the computer. For the applications described in this paper, $\epsilon = 10^{-8}$ is used.

Note that the Jacobian is very sparse and only the cells that contribute to the right hand side need to be perturbed. In 1D there are only three nonzero elements for each row i as explained earlier. The Jacobian for river networks can also be created using object oriented programming methods (Lal et al. 2005).

Numerical Experiments

Numerical experiments are carried out to test the TVDLF method and compare the results with the results obtained from commonly used diffusive wave models, analytical models, and data from a field experiment. When the TVDLF method is compared to other methods, only the numerical algorithms are compared. Most popular overland flow models use 2D versions of the nonlinear implicit method by Akan and Yen (1981). Since all numerical methods that satisfy the consistency condition give very similar solutions with fine discretizations, it is sometimes useful to compare numerical errors instead of numerical solutions.

The numerical experiments explained below consist of six steady-state experiments and five dynamic wave experiments each covering the nonlinear implicit method (Akan and Yen 1981), the noniterative implicit method (Lal 1998), and the TVDLF method. A grid convergence test is carried out to make sure that the solution converges to the true solution as the segment size and the time step get finer. Numerical error is also estimated for a problem that is similar to the field test problem in order to understand how the numerical error changes with the discretization.

Steady-State Experiment

The steady-state experiment is carried out with an ideal river with a uniform bed slope of s_0 and an upstream water depth of h_0 at $x = 0$. The steady-state solution for this problem obtained using the implicit TVDLF method is compared to the steady-state solution obtained using a more accurate fourth-order Runge-Kutta (RK4) method using a finer mesh.

The steady-state form of the governing Eq. (2) without inertia terms can be written using dimensionless variables as

$$\frac{\partial \hat{h}}{\partial \hat{x}} = -\left[1 - \left(\frac{1}{\hat{h}}\right)^{(1+\gamma)/\alpha}\right] \tag{25}$$

where $\hat{h} = h/h_n$; $\hat{x} = s_0 x/h_n$; h_n = normal depth. The solution of Eq. (25) gives a water surface profile similar to the M1 profile (Henderson 1966). Two steady-state profiles with $\hat{h}_0 = 2.0$ and $\hat{h}_0 = 5.0$ where $\hat{h}_0 = h_0/h_n$ are used in the comparison. The TVDLF method is applied using various spatial discretizations measured using N, where N = number of grid cells in the domain. A dimensionless discretization parameter is defined as $\phi = \Delta x s_0/h_n = Ls_0/(Nh_n)$ where L = length of the domain. The physical parameters used with the TVDLF test are $s_0 = 0.01$, $n_b = 0.03$, $h_n = 1.0$, and $L = 500.0$ m. The RK4 solution of the dimensionless problem is obtained with $N = 1{,}000$ and $\Delta x = 0.005$. Fig. 2 shows how the TVDLF solutions at steady state compare with the RK4 solution.

Grid Convergence Test

A grid convergence test is carried out for the TVDLF method with the same steady-state setup explained in the previous section with $\hat{h}_0 = h_0/h_n = 2.0$, assuming the RK4 solution of (25) to be accurate. The solutions at arbitrary locations $\hat{x} = 0.5$, 1.5, and 3.0 calculated as 1.57532, 1.0689, and 1.00054 are used to calculate the numerical errors of the implicit TVDLF method. Table 1 shows the numerical errors corresponding to different dimensionless discretizations Δx calculated as $\Delta x = L/N$, e.g., for $N = 10$, 20, 50. These values correspond to $\phi = 0.5$, 0.25, 0.1. These results can be used to show that the TVDLF solution converges to the RK4 solution with a first-order accuracy as Δx or ϕ becomes small. Fig. 2 shows some of the numerical solutions of $\hat{h}$.

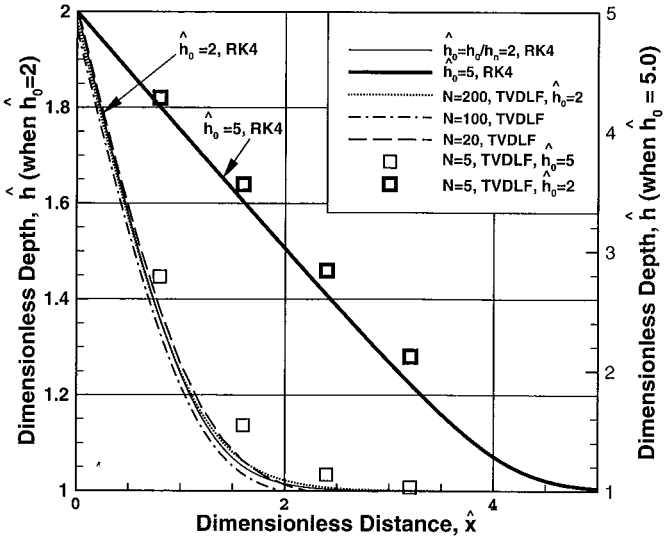

Fig. 2. Comparison of steady-state water levels obtained using the RK4 method and the TVDLF method

Table 1. Numerical Errors from Grid Convergence Test

N, Number grid points	ϕ	$\hat{x} = 0.5$	$\hat{x} = 1.5$	$\hat{x} = 3.0$
10	0.50	0.02986	0.06859	0.00757
20	0.25	0.01458	0.03550	0.00255
50	0.10	0.00571	0.01455	0.00073
100	0.05	0.00282	0.00731	0.00032
200	0.025	0.00139	0.00364	0.00015
500	0.010	0.00053	0.00141	0.00006

Wave Propagation Experiment

The purpose of this experiment is to compare the wave speeds and the logarithmic decrements of water waves simulated using three numerical methods and the analytical solutions. The experiment allows testing under both kinematic and diffusive wave conditions. The three methods tested are the fully implicit method (Akan and Yen 1981) explained using Eq. (8) under option (b), the noniterative implicit methods (Lal 1998) explained using Eq. (8) under option (c), and the TVDLF method explained using the flux function (9). Two-dimensional versions of first two methods are used in popular overland flow models.

Derivation of Analytical Solution

An analytical solution is obtained for a small amplitude sinusoidal water depth disturbance of amplitude h_* along the canal over time. This solution is imposed on the equilibrium depth (uniform flow depth) of h_n. A solution of the form $\mathbf{h}_* = h' e^{\mathbf{f}t - \mathbf{k}x}$ is sought for (4) by substituting $\mathbf{h}_*$ for h where $\mathbf{k} = k_1 + k_2\mathbf{I}$ and $\mathbf{f} = f_1 + f_2\mathbf{I}$ in complex form; $\mathbf{I} = \sqrt{-1}$; f_1 = the decay constant for time decay, assumed as 0; f_2 = frequency of the discharge wave introduced at upstream = $2\pi/P$; P = wave period; k_1 = spatial decay constant; k_2 = wave number = $2\pi/L$; L = wave length. The real part of $\mathbf{h}_*$ is used as the solution. The test is limited to continuous sinusoidal waves with no time decay introduced at the upstream. Substituting in Eq. (4),

$$\mathbf{f} - c\mathbf{k} = K\mathbf{k}^2 \tag{26}$$

Dimensionless variables are now defined as

$$\hat{\mathbf{k}} = \frac{\mathbf{k}h_n}{s_0}, \qquad \hat{\mathbf{f}} = \frac{\mathbf{f}h_n}{u_n s_0} \tag{27}$$

where h_n is obtained using Eq. (3) or $h_n = [Q_0 n_b/(Bs_0^{\alpha})]^{1/(1+\gamma)}$ for wide rectangular canal sections; Q_0 = canal discharge; B = width of the canal. Eq. (26) then becomes

$$\alpha\hat{\mathbf{k}}^2 + (1+\gamma)\hat{\mathbf{k}} - \hat{\mathbf{f}} = 0 \tag{28}$$

The analytical solution of $\hat{\mathbf{k}}$ is

$$\hat{\mathbf{k}} = \frac{-(1+\gamma) + \sqrt{(1+\gamma)^2 - 4\alpha\hat{\mathbf{f}}}}{2\alpha} \tag{29}$$

The solution of h_* can now be written as

$$h_* = h' e^{-k_1 x}\cos(f_2 t - k_2 x) \tag{30}$$

where h' = amplitude at $x = 0$. The wave speed is calculated as

$$\hat{c} = \frac{c}{u_n} = \frac{\hat{f}_2}{\hat{k}_2} \tag{31}$$

Table 2. Information Used in Creating Model Runs Shown in Table 3

$\hat{f}$	Period, P (s)	Δx (m)	Δt (s)	C_r	β_e
0.1	40668	100.1	50.0	0.257	0.299
0.5	8133	20.31	38.8	0.528	3.030
1.0	4066	10.56	19.4	0.946	10.439
5.0	813	3.077	3.88	0.649	24.590
10	407	2.033	1.94	0.491	28.180

Note: For numerical models, $s_0 = 0.001$, $h_n = 0.2$ m, $n_b = 0.035$.

and the logarithmic decrement that is used to measure the subsidence of a wave is calculated as

$$\hat{\delta} = 2\pi \frac{\hat{k}_1}{\hat{k}_2} \tag{32}$$

The dimensionless variables $\hat{\mathbf{f}}$ and $\hat{\mathbf{k}}$ are very useful in creating many benchmark tests representing a wide range of bed slopes and friction values. These tests are useful when comparing the three numerical methods. The variable $\hat{\mathbf{f}}$ determines if the flow is kinematic or diffusive, as described later.

Comparison of Numerical and Analytical Solutions

The three numerical methods described earlier are tested by comparing the numerical solutions against analytical solutions. The analytical solutions are obtained using Eq. (29) with $\hat{f} = 0.1$, 0.5, 1.0, 5.0, and 10. The numerical solutions are obtained using physical parameters $h_n = 0.2$ m, $s_0 = 0.001$, $n_b = 0.035$, and $u_n = 0.309$ m/s. The value of P for a given $\hat{\mathbf{f}}$ is calculated using $P = 2\pi h_n/(\hat{f} u_n s_0)$. Even if actual parameter values are reported here for completeness, results are presented only using dimensionless variables.

The time step Δt and the segment size Δx for the numerical models are selected to keep numerical errors under control. This is accomplished by keeping the values of dimensionless discretizations ϕ and ψ below 0.04. They are defined as (Hirsch 2007; Lal 2000)

$$\phi = k_2 \Delta x \quad \text{and} \quad \psi = f_2 \Delta t \tag{33}$$

The values of Δx and Δt are calculated as $\Delta t = \psi P/(2\pi)$ and $\Delta x = \phi h_n/(\hat{k}_2 s_0)$. The value of $\hat{c}$ from the model output is calculated using $L/(Pu_n)$. The value of the logarithmic decrement is calculated using $\hat{\delta} = \ln(h_p/h_{p+1})$ where h_p and h_{p+1} are successive wave peaks in the simulated solution at a given time. Table 2 shows the physical parameters and the Δx and Δt values used with the three numerical methods.

The values of Δt shown in the table are the time steps below which all the methods are stable and nonoscillatory. The fully implicit method and the TVDLF method do not need time step control for stability. However, the noniterative implicit method is stable only if $C_r < 1$ where $C_r = c\Delta t/\Delta x$ is the Courant-Friedrichs-Lewy (CFL) number; c is defined in Eq. (5). Stability does not depend on β_e for all methods where $\beta_e = K\Delta t/\Delta x^2$ = a dimensioness mesh ratio; K is defined in Eq. (4). Table 3 shows the analytical values of $\hat{c}$ and $\hat{\delta}$ obtained using Eqs. (29), (31), and (32), and the numerical values obtained using the three methods.

Fig. 3 shows snap shots of two of the actual water surface profile waves corresponding to $\hat{f} = 0.1$ and 10 in starting the beginning of a cycle at $x = 0$. For the plots shown, $h_n = 0.2$ m and $h' = 0.02$ m are used. The amplitude envelopes are shown in dotted lines. The purpose of Fig. 3 is to show different waves in actual dimensions in a single plot. The wave for $\hat{f} = 10$ is diffusive and decays rapidly while the wave for $\hat{f} = 0.1$ is kniematic and decays slowly. Only a portion of the $\hat{f} = 0.1$ is visible because the wave is long. The plots for all three numerical methods and the analytical solution almost coincide for the discretizations chosen in Table 3. Fig. 3 and Table 3 show that as $\hat{f}$ becomes very small and the flow becomes kinematic, all numerical solutions start to deviate from the exact solution.

Results of this experiment show that while iterations are not required for the TVDLF method, many iterations are needed for the fully implicit method. In the case of the current benchmark, the number of iterations needed is about 2–3 per time step. Considering that the basic difference between the noniterative method and the TVDLF method is the addition of the flux correction term in the TVD method, it is clear that the flux correction term is the reason for stability of the TVDLF method with steep slopes.

The analytical solution (29) used here is useful beyond testing numerical methods. It can also be used to identify if a given no inertia problem is kinematic or diffusive in nature. If the value of $\hat{f}$ is much smaller than 1, the root $\hat{k}$ of Eq. (29) is mostly imaginary, and the flow is kinematic with negligible wave decay with time and distance. If $\hat{f}$ is much larger than 1, the flow is diffusive with a significant wave decay behavior. The condition of applicability of the kinematic model given as $Ps_0u_n/h_n > 171$ (Ponce et al. 1978) can also be expressed using the dimensionless parameter $\hat{f}$ as $\hat{f} < 0.037$ for the purposes of comparison. The condition of applicability of the diffusive wave model when the inertia terms are negligible, $Ps_0\sqrt{g/h_n} > 30$, can be expressed similarly as $\mathrm{F}\hat{f} < 21$ where F = Froude number. Even if the numerical limits 0.037 and 21 listed here do not directly apply for the current problem, which has continuous sinusoidal discharge pulses sent from upstream instead of time decaying pulses, this exercise demonstrates the use of $\hat{f}$ in identifying kinematic and diffusive flow types. Table 3 shows how the experiments can be designed to cover both kinematic and diffusive problems.

Field Experiment at Dambulu River in Sri Lanka

A field experiment was carried out in the Dambulu River of Sri Lanka to verify the applicability of the implicit TVDLF method to steep river flow problems. The Dambulu River starts at 7°52′15.85″N and 80°37′51.75″E, near the famous Cricket Stadium at Dambulla, and ends at the historic Kala-Wewa Reservoir

Table 3. Comparison of Results of Three Numerical Methods with Analytical Solutions

$\hat{f}$	$\hat{c}$ Analytical (m)	$\hat{c}$ (Akan)	$\hat{c}$ (Noniterative implicit)	$\hat{c}$ (TVDLF)	$\hat{\delta}$ Analytical	$\hat{\delta}$ (Akan)	$\hat{\delta}$ (Noniterative implicit)	$\hat{\delta}$ (TVDLF)
0.1	1.6674	1.664	1.667	1.674	0.113	0.139	0.090	0.232
0.5	1.6926	1.709	1.689	1.719	0.553	0.643	0.507	0.728
1.0	1.7607	1.764	1.742	1.781	1.041	1.109	0.965	1.182
5.0	2.5648	2.497	2.476	2.564	2.895	3.093	3.053	3.194
10	3.3889	3.437	3.285	3.306	3.667	3.867	3.438	3.332

Note: Analytical using Eqs. (31) and (32); Akan = Akan and Yen (1981); noniterative implicit Lal (1998).

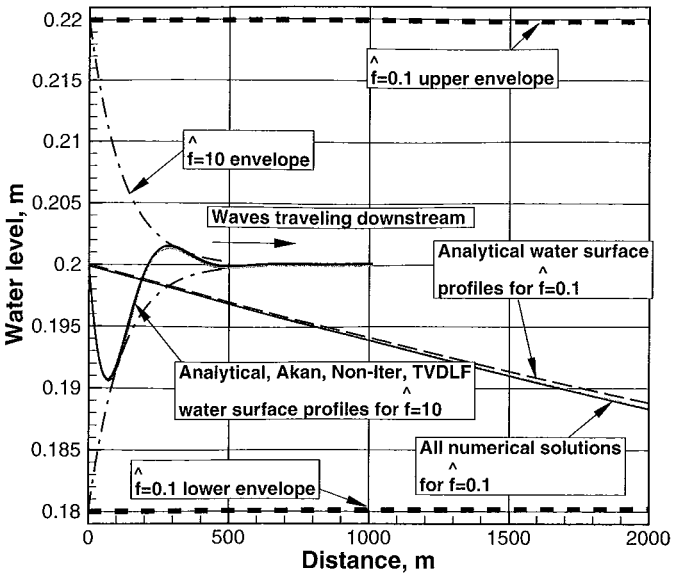

Fig. 3. Results of the wave propagation test for $\hat{f} = 0.1$ and $\hat{f} = 10$ shown in Table 3

built during 500 AD. The 17.5-km test reach begins at the Dambulu reservoir, which has the outflow structures necessary to create a design hydrograph of any given shape. The first 4.0 km of the river has a slope of 0.0075, and the next 13.5 km has a slope of 0.00153.

A discharge hydrograph of sinusoidal shape and a period of 6 h was created at the upstream end of the reservoir by manipulating the control gates. The discharge rates were estimated based on precise rotations of the gear wheels and rating curves. The discharge was kept at $Q = 17.0$ m^3/s for $t < 7.0$ h, and $Q = 17.0 + 8.49 \sin[2\pi(t - 7.0)/6.0]$m^3/s for $t > 7.0$ h, where $t = 00{:}00$ h on January 12, 2008, Colombo time. The peak discharge rate was 25.48 m^3/s (900 cfs), e.g., at times 8:30 a.m., 2:30 p.m., and the trough discharge rate was 8.49 m^3/s (300 cfs), e.g., at times 11:30 a.m., 5:30 p.m.. The sinusoidal shape made it possible to estimate analytical solutions and numerical errors to this problem assuming the bed slope to be constant. However, true bed topography is used for all other model simulations.

Fig. 4 shows a location map of the river, the Dambulu Reservoir, and the gage G1 at the upstream end. Gage G2 at the Kiralawa bridge and G3 at the Udanigama village are at distances 7.5 km and 10.9 km, respectively, along the river. Fig. 5 shows a picture of the rapids section of the river. The alluvial section of the river starts at 15 km, and the river ends at around 17.5 km.

An implicit TVDLF method is used to simulate the flow in the river resulting from the sinusoidal discharge variation at the upstream end. The river is discretized into 175 segments that are approximately 100 m long. The time step used is 1 min. The river is 10 m to 100 m wide, and has an average width of 37.0 m. The Manning's roughness is calibrated using a least square method. The values obtained for the 0-7.5 km, 7.5-10.9 km, and 10.9-17.5 km river stretches are 0.083, 0.045, and 0.065, respectively. Fig. 6 shows that the water levels calculated using the TVDLF method compare well with the water levels observed in the field even when some of the data collection methods were crude. Data collection was hampered by the limited amount of access available for setting up the initial conditions, poor terrain, and wild elephants.

The field data can be used to calculate the speed of the wave as $c_{obs} = 0.83$ m/s by noting that it took about 2.5 h for the wave peak to travel 7.5 km up to G2. To obtain an analytical estimate of the same, the uniform depth h_n is calculated as $h_n = [Q_0 n_b/(B\sqrt{s_0})]^{0.6} = 0.98$ m using canal discharge $Q_0 = 17$ m^3/s, width $B = 37$ m, $s_0 = 1.53 \times 10^{-3}$, $n_b = 0.083$. The uniform flow velocity $u_n = Q_0/(h_n B) = 0.47$ m/s. The value of $\hat{f} = f_2 h_n/(u_n s_0) = 0.40$, indicating that the flow is kinematic according to Eq. (29). For kinematic flow, u_n can be used to calculate an analytical estimate for wave speed using Eq. (5) as $c_{anl} = u_n(1 + \gamma) = 0.78$ m/s which can be compared to the observed speed of 0.83 m/s. These results show that some of the basic behaviors of the river can be predicted using simple calculations.

Numerical Error

When numerical methods are unconditionally stable as in the case of the fully implicit method by Akan and Yen (1981), the TVDLF method, or the noniterative method, there is a tendency for some users to use large time steps ignoring the numerical error associated with it. Fortunately, this problem is not significant in the case of explicit methods where the CFL condition places some limits on the time step and therefore the numerical error.

In the absence of clear guidelines for error control, it is important to understand how the amplitude and phase errors in a solution vary with the discretization. The example of the Dambulu River is

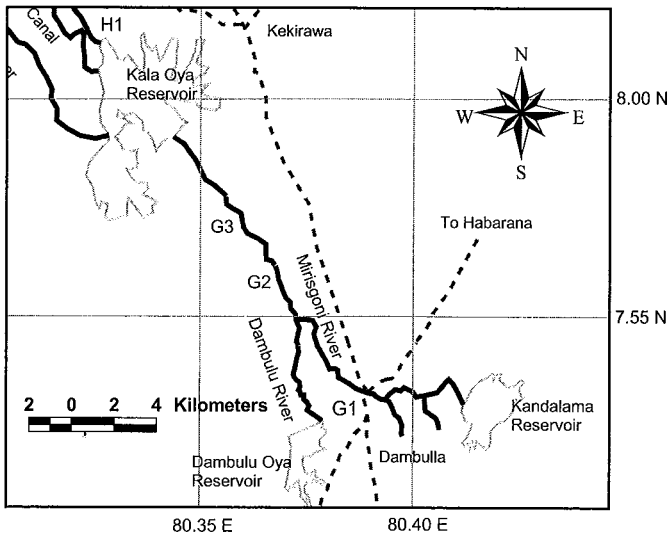

Fig. 4. Map of the test site in Dambulla, Sri Lanka

Fig. 5. Upstream section of Dambulu River, Sri Lanka (image by Wasantha Lal)

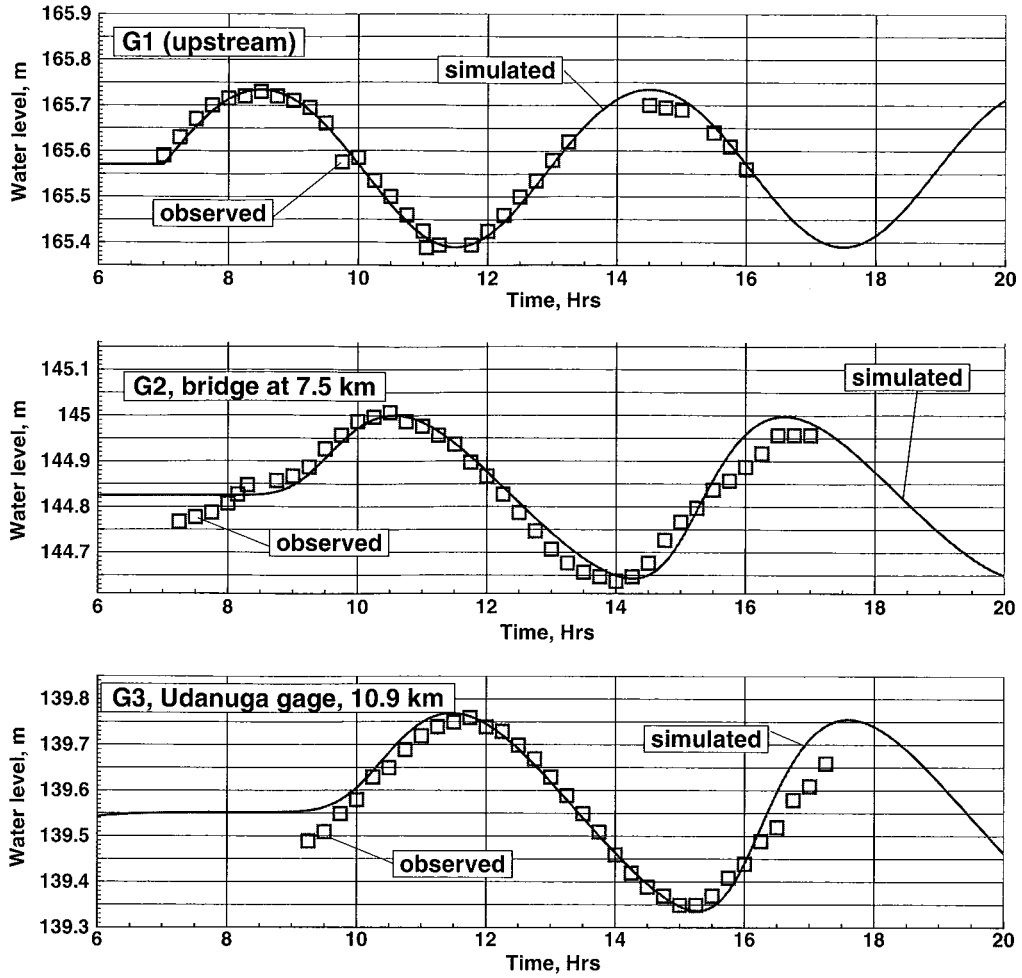

Fig. 6. Observed water levels at gages G1, G2, and G3 along Dambulu River compared with water levels simulated using the TVDLF method

used to understand this problem. For this purpose, the error in the amplitude and the phase are calculated using

$$\epsilon_a = \frac{a_n - a_a}{a_a}; \qquad \epsilon_\varphi = \frac{\varphi_a - \varphi_n}{P} \tag{34}$$

where a_n, φ_n = the amplitude and the phase of the numerical solution; a_a, φ_a = amplitude and the phase of the analytical solution; P = wave period. The analytical solution is obtained using Eq. (29).

When calculating the numerical error in the TVDLF solution for Dambulu River water levels, the only way to obtain an analytical solution is to assume that the river bed has a flat bottom approximating the true bottom. For this river, $s_0 = 0.00153$ and $n_b = 0.083$ are assumed, making it possible to obtain $u_n = 0.47$, $h_n = 0.98$, F = Froude number = 0.15, and the wave length as 16.8 km. Fig. 7 shows how the amplitude and the phase errors of the water levels at gage G3 simulated using the TVDLF method and defined using Eq. (34) vary with C_r and ϕ where ϕ is defined using Eq. (33). C_r and ϕ represent dimensionless forms of Δt and Δx that are also shown in Table 4. The results show that both amplitude and phase errors are generally negative and the error magnitudes increase with Δx and Δt. According to this experiment, model results are not affected much whether the Jacobian is calculated analytically using Eqs. (21) and (22) or numerically using Eq. (24).

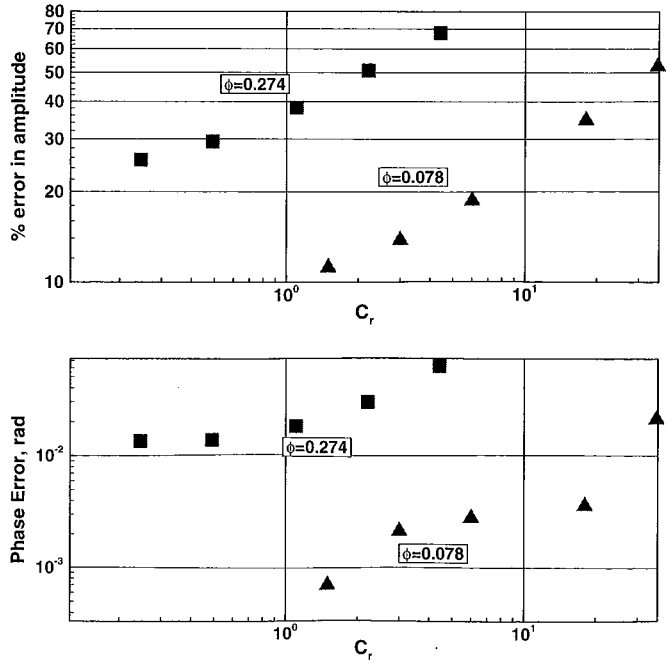

Fig. 7. Amplitude and phase errors of water levels obtained for Dambulu River at 10.9 km using the TVDLF method

Table 4. Approximate Numerical Errors of TVDLF Solution for Dambulu River at 10.9 km from Upstream

Δx, m	Δt, s	ψ	C_r	β	ϵ_a	ϵ_ϕ
	100.0	0.029	0.22	0.24	25.5%	0.0134
350	200.0	0.058	0.44	0.49	29.4%	0.0137
350	450.0	0.131	1.00	1.10	38.1%	0.0180
350	900.0	0.261	2.00	2.20	50.8%	0.0295
350	1800.0	0.523	4.00	4.41	67.7%	0.0625
100	50.0	0.014	0.39	1.50	11.2%	0.0007
100	100.0	0.029	0.78	3.00	13.8%	0.0021
100	200.0	0.058	1.55	6.00	18.7%	0.0058
100	1200.0	0.349	9.33	36.03	52.5%	0.0211
100	2400.0	0.698	18.66	72.07	73.6%	0.0730

Note: For this error analysis, $s_0 = 0.00153$, $u_n = 0.47$ m, $h_n = 0.98$ m, $\mathsf{F}_r = 0.15$, $\Delta x = 350$ m ($\phi = 0.274$), and $\Delta x = 100$ m ($\phi = 0.078$) are assumed.

Table 5. Approximate Numerical Errors of Problem in Table 4

Δx, m	Δt, s	ψ	C_r	β	ϵ_a	ϵ_ϕ
100	50.0	0.014	0.39	1.50	24.6%	0.0080
100	200.0	0.058	1.56	6.06	16.7%	0.0109
100	600.0	0.174	4.66	18.01	−10.2%	0.0121
100	2400.0	0.698	18.66	72.07	−72.8%	0.0259

Note: When using second-order accurate flux function with TVDLF method. For this error analysis, $s_0 = 0.00153$, $u_n = 0.47$ m, $h_n = 0.98$ m, $\mathsf{F}_r = 0.15$, and $\Delta x = 100$ m ($\phi = 0.078$) are assumed.

Table 6. Approximate Numerical Errors When Using First-Order TVDLF Method When Bed Slope is Arbitrarily Steep

Δx, m	Δt, s	ψ	C_r	β	ϵ_a	ϵ_ϕ
100	150.0	0.044	4.63	0.045	1.0%	0.00026
100	300.0	0.087	9.28	0.090	3.1%	0.00014
100	600.0	0.174	18.57	0.090	7.8%	0.00021
100	1200.0	0.349	37.14	0.360	15.9%	0.00280

Note: For this error analysis, $s_0 = 0.153$, $h_n = 0.25$ m, $u_n = 1.86$ m/s; $\mathsf{F} = 1.2$, and $\Delta x = 100$ m ($\phi = 0.00015$) are assumed.

Table 5 shows the numerical error in the same problem when a second-order accurate flux function is used instsead of a first-order accurate flux function as in all other cases. The second-order accurate flux function used here is described using Eqs. (11)–(13). Table 5 shows that the numerical error of the second-order method is smaller, but only with small discretizations.

Table 6 shows the numerical error in a similar problem, but with a bed slope that is 100 times larger. The objective here is to find out if the method is still stable, and how the error varies with the time step. The physical parameters used here are $s_0 = 0.153$, $u_n = 1.86$, $h_n = 0.25$, $\mathsf{F} = 1.19$, and wave length is 66.9 km. This experiment creates kinematic flow conditions due to the steep slope. The results show that the implicit TVDLF method is stable even with large CFL numbers C_r. The results also show that the numerical errors are small for this problem because the wave length is large, and therefore ϕ is small. Results of this and other experiments show that the implicit TVDLF method is stable when the bottom slope is steep.

Conclusions

The development and the application of an implicit TVDLF method to solve the diffusive wave approximation of the St. Venant equations is presented in this paper. Tests are carried out to show that the solutions obtained using the method for both steady-state and unsteady-state problems compare well with same solutions obtained with the existing fully implicit method (Akan and Yen 1981), the noniterative implicit method (Lal 1998), and the analytical solutions.

A backwater problem that has a solution similar to the M1 profile is used for the steady-state test. The solution obtained using the fourth-order Runge-Kutta method (RK4) is used as the benchmark solution. Results show that the TVDLF and RK4 solutions agree well with each other for two steady-state problems. This test is also extended as a grid convergence test. Results of this test show that the TVDLF solution converges to the true solution as the discretization is refined.

A wave propagation problem that has an analytical solution is used next as an unsteady-state test. Wave speeds and wave decays of various numerical methods are investigated in this test. Results show that all the methods give solutions that compare well with the analytical solutions. These results also show that the TVDLF method and the fully implicit method (Akan and Yen 1981) are stable with very large time steps, while the noniterative method (Lal 1998) is not. The TVDLF method, however, does not require iterations, while the fully implicit method requires many iterations depending on the problem. The TVDLF method gives good results for a wide range of kinematic, diffusive, and mixed-flow conditions, and a wide range of wave frequencies except when the inertia terms are significant.

A field experiment carried out in a steep, 17.5-km long section of the Dabulu River of Sri Lanka was used to demonstrate that the TVDLF method can simulate the movement of artificially generated water waves with a period of 6 h. Results show that the numerical solutions agree well with the field observations.

The same field problem is used as the basis for carrying out numerical experiments that can be helpful in understanding the behavior of the numerical error when the spatial and temporal discretizations are varied. The results of this test can be useful in the future when selecting mesh sizes and time steps to keep the numerical error under control.

Acknowledgments

The authors wish to thank Joel VanArman, Zaki Moustafa, Randy Vanzee, Raul Novoa, Sharika Senarath, and Walter Wilcox at the South Florida Water Management District, West Palm Beach, Florida, for reviewing the manuscript and making valuable comments. The authors also wish to thank Mr. J. A. S. A. Jayasinghe, (Director River Basins), Mr. B. S. Layanagama (Deputy Director), Mr. Nilantha Dhanapala (Chief Engineer), and Mr. W. K. Jinadasa (IT Manager) of the Mahaweli Authority of Sri Lanka for supporting the field experiment at the Dambulu River in Sri Lanka.

References

Akan, A. O., and Yen, B. C. (1981). "Diffusion-wave flood routing in channel networks." *J. Hydr. Div.*, 107(6), 719–731.

Graham, D. N., and Butts, M. B. (2005). "Flexible integrated watershed modeling with MIKE SHE." *Watershed Models*, V. P. Singh and D. K. Frevert, eds., CRC Press, Boca Raton, FL, 245–272.

Harten, A. (1983). "High resolution method for hyperbolic conservation laws." *J. Comput. Phys.*, 49, 357–393.

Henderson, F. M. (1966). *Open channel flow*, MacMillan, New York.

Hirsch, C. (2007). *Numerical computation of internal and external flow*, Wiley, New York.

Hromadka, T. V., II, McCuen, R. H., and Yen, C. C. (1987). *Computational hydrology in flood control design and planning*, Lighthouse.
Kadlec, R. H., and Wallace, S. T. (2009). *Treatment wetlands*, 2nd Ed., CRC Press, Boca Raton, FL.
Lal, A. M. W. (1998). "Weighted implicit finite-volume model for overland flow." *J. Hydraul. Eng.*, 124(4), 342–349.
Lal, A. M. W. (2000). "Numerical errors in groundwater and overland flow models." *Water Resour. Res.*, 36(5), 1237–1247.
Lal, A. M. W. (2008). "Development of a robust diffusion-kinematic flow algorithm for regional models operating with large time steps." *EWRI World Env. and Water Res. Conf.*, ASCE, Honolulu, HI.
Lal, A. M. W., Van Zee, R., and Belnap, M. (2005). "Case study: A model to simulate regional flow in south Florida." *J. Hydraul. Eng.*, 131(4), 247–258.
Ponce, V. M. (1991). "The Kinematic Wave Controversy." *J. Hydraul. Eng.*, 117(4), 511–525.
Ponce, V. M., Li, R. M., and Simons, D. B. (1978). "Applicability of Kinematic and Diffusion Models." *J. Hydr. Div.*, 104(3), 353–360.
Rodriguez, L. B., Cello, P. A., Vionette, C. A., and Goodrich, D. (2008). "Fully conservative coupling of HEC-RAS with MODFLOW to simulate stream-aquifer interactions in a Drainage Basin." *J. Hydrol.*, 353(1–2), 129–142.
Rosner, L. A., Shubinski, R. P., and Aldrich, J. A. (1984). "Stormwater management model user's manual version III, addendum I EXTRAN." *EPA-600/2-84-109b*, U.S. Environmental Protection Agency, Cincinnati, OH.
Singh, V. P. (1996). *Kinematic wave modeling in water resources*, Wiley-IEEE, New York.
Toth, G., Keppens, R., and Botchev, M. A. (1998). "Implicit and semi-implicit schemes in the versatile advection code: Numerical tests." *Astron. Astrophys.*, 332, 1159–1170.
Toth, G., and Odstrcil, D. (1996). "Comparison of some flux corrected transport and total variation diminishing numerical schemes for hydrodynamic and magneto hydrodynamic problems." *J. Comput. Phys.*, 128, 82–100.
van Leer, B. (1979). "Towards the ultimate conservative difference scheme. V. A second-order sequel to Godunov's method." *J. Comput. Phys.*, 32(1), 101–136.
Yee, H. C. (1987). "Construction of explicit and implicit symmetric TVD Schemes and their applications." *J. Comput. Phys.*, 68(1), 151–179.
Yee, H. C. (1989). "A class of high-resolution explicit and implicit shock-capturing methods." *NASA Technical Memorandum 101088*, NASA Ames Research Center, Moffette Field, CA.